Nucleation and growth dynamics across the antiferromagnetic to ferromagnetic transition in $(Fe_{0.975}Ni_{0.025})_{50}Rh_{50}$: analogy with crystallization

2008 J. Phys.: Condens. Matter 20 325208

(http://iopscience.iop.org/0953-8984/20/32/325208)

J. Phys.: Condens. Matter **20** (2008) 325208 (7pp) doi:10.1088/0953-8984/20/32/325208

Nucleation and growth dynamics across the antiferromagnetic to ferromagnetic transition in $(Fe_{0.975}Ni_{0.025})_{50}Rh_{50}$: analogy with crystallization

Meghmalhar Manekar and S B Roy

Magnetic and Superconducting Materials Section, Raja Ramanna Centre for Advanced Technology, Indore 452 013, India

Received 18 March 2008, in final form 19 June 2008
Published 9 July 2008
Online at stacks.iop.org/JPhysCM/20/325208

Abstract

We present the results of ac susceptibility and dc magnetization measurements on polycrystalline $(Fe_{0.975}Ni_{0.025})_{50}Rh_{50}$. The sample undergoes a first order antiferromagnetic to ferromagnetic transition both as a function of temperature and magnetic field. The presence of phase coexistence and metastable states across the transition is highlighted through the observation of minor hysteresis loops and magnetic relaxation respectively. The magnetic relaxation follows a power law which can arise due to long-range dipolar interaction between the ferromagnetic clusters in the phase coexistent state. The non-monotonic behaviour of the power law exponent as a function of temperature and magnetic field suggests a nucleation and growth behaviour very similar to crystallization of solids. The area of minor hysteresis loops is conjectured to be related to the phase fraction of one of the phases involved in the transition. The temperature and field dependent phase fraction is shown to follow the well known Avrami law of transformation kinetics.

(Some figures in this article are in colour only in the electronic version)

1. Introduction

Nucleation and growth dynamics during transformations in solids has been a subject of great interest [1]. The solidification and melting transitions are known to be of a first order nature and attempts have been carried out to establish the common features of such transitions with first order transitions in other systems. In this direction, it has been shown that the vortex lattice in a type-II superconductor melts like ice melting to water [2]. Many studies using local imaging at various length scales have been carried out on diverse systems to study the transformation kinetics across first order magneto-structural transitions [3–10]. While it is relatively straightforward to estimate the phase fractions of the coexisting phases using local imaging [11], it is quite difficult to get a physical parameter from bulk measurements which can be related to the phase fraction. In situations where the local imaging or measurement of latent heat is difficult, due to their small values, hysteresis across the transition is used to determine the first order nature of the transition [12]. The presence of minor hysteresis loops (MHL) is usually taken as a signature of phase coexistence of both the phases across a first order transition [13]. However the correlation between the area of MHL and the phase fraction has only been intuitive for various systems [14]. In this work we attempt to correlate the area of MHLs with the phase fraction by studying the first order magnetic transition from the antiferromagnetic (AFM) state to the ferromagnetic (FM) state in polycrystalline $(Fe_{0.975}Ni_{0.025})_{50}Rh_{50}$ using bulk ac susceptibility and dc magnetization measurements. Time dependent magnetization measurements confirm the presence of metastable states across this first order transition. The results of these relaxation measurements are used to draw an analogy between the dynamics of this first order transition with the generalized model of crystallization of solids. The inferred phase fraction from the areas of MHLs appears to follow the well known Avrami law for phase transformation in solids [15].

The parent Fe–Rh alloy system has been widely studied due to the giant magnetocaloric effect [16], giant elastocaloric effect [17], giant magnetostriction [18] and giant

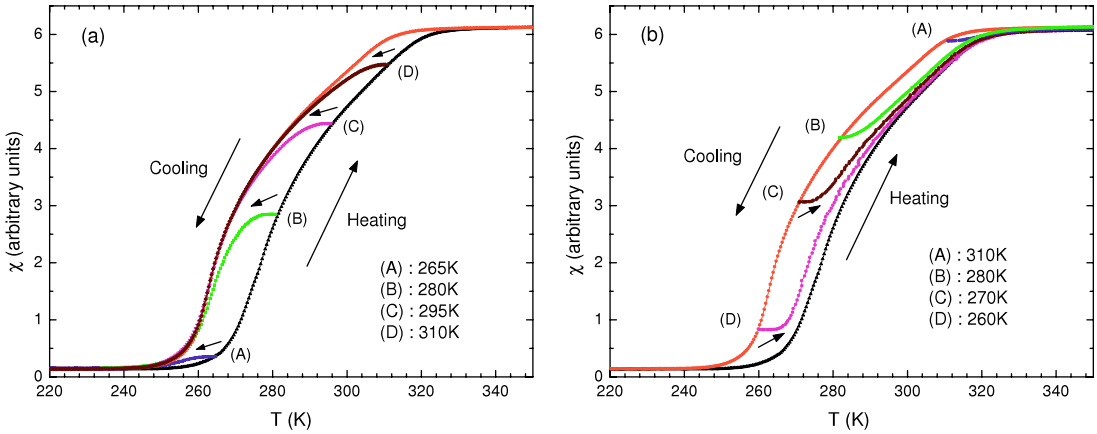

Figure 1. Ac susceptibility as a function of temperature. (a) Minor hysteresis loops initiated on the heating cycle and (b) minor hysteresis loops initiated on the cooling cycle. The temperatures of initiation of the minor loops in both cases are marked as A, B, C and D.

magnetoresistance [19] occurring close to room temperature. Such wide range of functionality for this alloy system is thought to arise due to a first order magnetic transition from an AFM to FM state which takes place both as a function of temperature (T) [20] and magnetic field (H) [21]. The addition of a small amount of Ni shifts the AFM to FM transition to lower temperatures and magnetic fields [22]. This well studied AFM to FM transition thus provides an interesting case study to understand the nucleation and growth dynamics across a first order magnetic transition. We first establish the generic features seen across a first order transition like phase coexistence and metastability for this AFM to FM transition. Next we try to draw an analogy between the nucleation and growth dynamics observed during a general solidification process with that during the AFM to FM transition.

2. Experimental details

A polycrystalline sample of (Fe, Ni)Rh was prepared by melting Fe, Ni and Rh having purities of 99.99%, 99.99% and 99.9%, respectively in an argon arc-melting furnace. The alloy button was remelted several times to ensure homogeneity. The alloy was later subjected to the following heat-treatment schedule: 48 h at 1100 °C, cooled to 800 °C at the rate of 2 °C min^{-1}, maintained for 24 h at 800 °C and then cooled to room temperature at the rate of 2 °C min^{-1}. This annealing schedule is similar to the one followed in case of $FeRh_{1-x}Pt_x$ alloys [23]. We have earlier used the same sequence in case of Fe–Rh alloy [3, 24] and found that the alloy shows reproducible magnetization behaviour even after numerous cyclings across the first order transition, which is unlike the case of the quenched sample [16]. Energy dispersive spectroscopy (EDS) confirmed the sample to be homogeneous with a composition of $(Fe_{0.975}Ni_{0.025})_{50}Rh_{50}$. Ac susceptibility was measured as a function of temperature using home-made apparatus [13]. The field was 3.4 × 10^{-4} T rms and the frequency was 333 Hz. Magnetization (M) measurements were performed as a function of T, H and time (t) using a commercial vibrating sample magnetometer (VSM, Quantum Design).

3. Results and discussion

Figure 1 shows the ac susceptibility as a function of T both during heating and cooling the sample respectively. A sharp rise in susceptibility slightly above 260 K during heating indicates the onset of the AFM to FM transition. During cooling, the onset of the FM to AFM transition takes place at T slightly below 320 K and the temperature dependent susceptibility shows a hysteresis across the transition. Hysteresis across the AFM to FM transition in Ni doped Fe–Rh alloys has been observed earlier in transport measurements [22]. Those results, along with the present ac susceptibility results, confirm the first order nature of the transition. Hysteresis across a first order transition occurs due to supercooling and/or superheating of the parent phase in the product matrix across the transition [12, 25]. As mentioned in our earlier reports on ac susceptibility measurements on other systems [13, 26] using the same apparatus, we have swept the temperature unidirectionally instead of stabilizing at each measurement point. This was done to avoid any thermal oscillation around the temperature set-point which is typical of any PID controller. Reversing the direction of temperature change before reaching the reversible region results in a minor loop. A minor loop which exhibits finite hysteresis is an indication of the coexistence of the two competing phases involved in the transition [13]. Thus a MHL initiated on the heating cycle indicates the coexistence of the growing product FM phase within the parent AFM phase. Similarly the MHLs initiated on the cooling cycle indicate the coexistence of the product AFM phase within the parent FM phase. Figures 1(a) and (b) show a few representative MHLs initiated both on the heating and the cooling cycle respectively. It can be seen that the area of MHLs increases while the sample transforms from one phase to another, indicating the growth of the product phase. We shall come back to this issue when we later attempt to quantify this area in terms of the phase fraction of the product phase involved in the transition.

Having established the presence of hysteresis and phase coexistence across the transition, we focus on another signature of a first order transition which is the existence of metastable

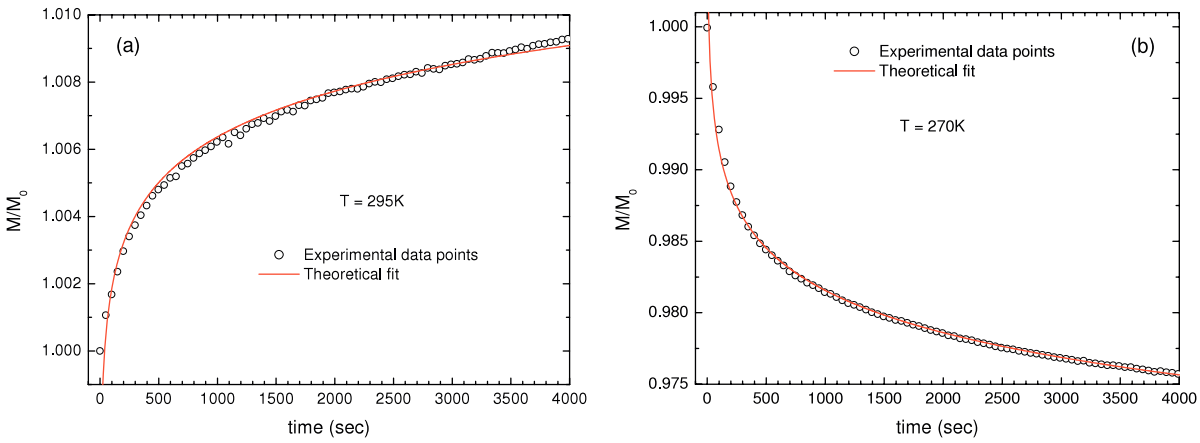

Figure 2. Time dependent magnetization during the temperature driven transition at representative temperatures on (a) the temperature increasing cycle and (b) the temperature decreasing cycle. Measurements were performed in a constant field of 100 Oe. Solid line shows the calculated curve from equation (1). See text for details.

states. The signature of metastable states can be experimentally observed by measuring the time dependence of a physical quantity intrinsic to the sample which is relevant to the phase transition. In this case, we measure the time dependence of magnetization at various temperatures in a fixed field of 100 Oe using the VSM.

Figure 2(a) shows normalized M as a function of time at 295 K on the heating cycle. The sample was heated unidirectionally up to 295 K from a temperature well below those values where the magnetization is reversible. The magnetization was then measured as a function of time immediately after the temperature was stabilized. The normalization of M is carried out with respect to M_0, which is the magnetization value at the first measurement point after reaching this temperature (i.e. at $t = 0$). The magnetization relaxes towards a higher value which clearly indicates the presence of a metastable (superheated) AFM phase relaxing towards the stable FM phase. The time dependent magnetization does not follow the usual exponential law but can be very well fitted with the following equation:

$$M/M_0 = -1 + 2t^{\gamma}. \tag{1}$$

The value of γ indicates the extent of relaxation, i.e. a higher value of γ means a greater degree of relaxation for the same time interval. This equation has been shown to apply to the relaxation of ferromagnetic dots which interact through long-range dipolar interaction [27]. A similar situation could arise for the case of an AFM to FM transition when the nucleation is heterogeneous. The clusters of the FM phase nucleate in the AFM matrix and these FM clusters can interact through a long-range dipolar interaction. By imaging the AFM to FM transition on a sub-micron scale in Fe–Rh alloy using magnetic force microscopy (MFM) [3], we have indeed shown the nucleation of the FM phase in the AFM matrix. Nucleation of the FM phase across the AFM to FM transition has been shown in various cases at different length scales (see [3–7]) highlighting the generality of the phenomenon. We believe that a similar phenomenon of nucleation takes place in our sample

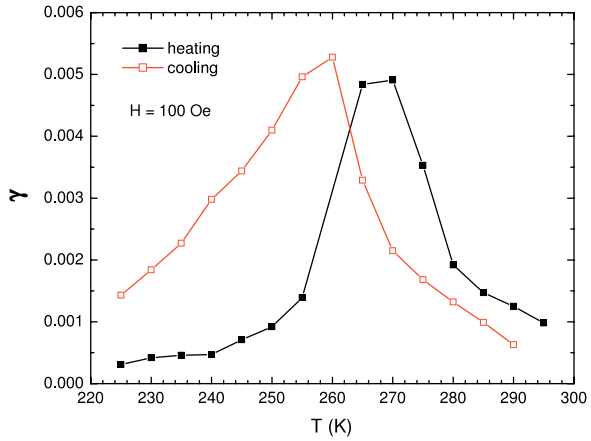

Figure 3. Temperature dependence of the exponent γ in equation (1) during the temperature driven transition. The absolute value of γ for the cooling cycle is plotted for the sake of comparison on the same scale.

and that the nucleated FM clusters interact through long-range forces.

Similar measurements of the time dependence of magnetization were performed on the cooling cycle as well. Figure 2(b) shows normalized M as a function of time at 270 K on the cooling cycle. Once again the relaxation can be described by the power law expressed in equation (1) with the value of γ being negative. To get the temperature dependence of γ, relaxation measurements were performed at various temperatures both during the heating and cooling cycle. To measure the relaxation during the heating (cooling) cycle, the temperature was increased (decreased) unidirectionally until the target value starting from the temperature where the magnetization is reversible.

Figure 3 shows the variation of the exponent γ in equation (1) as a function of temperature. While the value of γ is directly taken for the heating cycle, the magnitude of γ is plotted for the cooling cycle. During the heating cycle, the value of the exponent shows an initial increase with rise in

temperature and then drops with a further rise in temperature. This probably indicates that the initial part of the transition, while heating, is dominated by the creation of newer FM nuclei (giving rise to more relaxation) and in the later stages these nuclei merge to grow into the product FM phase. The peak in the temperature dependence of γ thus indicates the cross-over from nucleation to growth of the product phase. The same discussion applies to the temperature dependence of γ while cooling. The initial part of the cooling cycle appears to be dominated by the creation of newer AFM nuclei (resulting in a more rapid fall of magnetization) and later these AFM nuclei coalesce to form the low-temperature AFM phase.

The results of figure 3 indicate a nucleation and growth mechanism quite similar to that of the crystallization of solids described in the Avrami model [15]. The central assumption of the Avrami model is that the new phase is nucleated by *germ nuclei* which already exist in the parent matrix. The density of these germ nuclei diminishes through activation of some of these into growth nuclei and the coalescence of these nuclei in to the product phase. The nucleation events are considered to be random and the nuclei are allowed to freely overlap with each other during the growth process. The time dependent phase fraction of the product phase is then given by

$$f = 1 - \exp(-kt^{\eta}) \tag{2}$$

and is popularly known as the Kolmogorov–Johnson–Mehl–Avrami (KJMA) relation. Here k is related to the activation energy and η is known as the Avrami exponent which depends on the geometrical factors. The model was originally proposed for time dependent isothermal cases where the melt (liquid phase) has been sufficiently undercooled to enable crystallization of the solid phase.

If we extend this analogy for temperature driven first order magnetic transitions with the same assumption of nucleation and growth process, we should be able to (intuitively) see a similar relation of the temperature dependence of the phase fraction of the product phase. From the results of local imaging presented for field induced transitions in the case of Gd_5Ge_4 [5] and $CeFe_2$ based alloy systems [6], the nucleation and growth process appears to closely follow the assumptions of the Avrami model. We believe that similar nucleation and growth process takes place across the first order transition in the case of our alloy system under consideration.

The central issue now is to identify a proper parameter from bulk magnetization measurements which can be related to the phase fraction of the respective phases. The value of magnetization or susceptibility at a particular temperature cannot be directly taken as a measure of phase fraction because the nucleation of the FM phase is random, which leads to the magnetization of FM clusters aligning in random directions. The measured bulk magnetization is the vector sum of all these magnetic moments and thus will give an entirely different value of phase fraction. Through imaging of the magneto-structural transition using MFM, we have explicitly shown that the alignment of all the newly formed FM clusters during the transition is not along the same direction [3]. Also the time dependent magnetization data presented in figure 2 follow an entirely different equation to the Avrami model. This strongly indicates that bulk magnetization cannot directly be taken as a measure of phase fraction.

We propose that the area of MHLs can be a convenient parameter which is related to the phase fraction. Our heuristic argument is as follows. The envelope curve is the hysteresis curve which encloses both the reversible low-temperature and high-temperature phases. During the heating cycle of the envelope curve, the entire sample transforms from the AFM to FM phase. Similarly, the cooling curve represents the entire sample transforming from the FM to AFM phase. If a minor loop is initiated at any intermediate temperature value, it exhibits a smaller hysteresis compared to the hysteresis obtained on the complete envelope curve. A minor loop shows hysteresis when both the phases involved in the transition coexist. The MHL A of figure 1(a) encloses a smaller area compared to MHL B as the amount of FM phase at lower temperatures is lower during the heating cycle. Thus the growing FM fraction is also accompanied by a growing area of MHL. If we (hypothetically) divide the entire sample into smaller volumes, each hysteresis loop (envelope curve or MHL) can be thought of as a superimposition of smaller hysteresis loops for each of these volumes. Thus the area of the hysteresis loop initiated at any temperature, which is an addition of smaller hysteresis loops, would represent the volume of the transformed phase at that temperature. If we take the area of envelope curve as unity, the area of each MHL divided by the area of the envelope curve can then be taken as the phase fraction of the product phase at the temperature of initiation of MHL. A similar situation has been dealt with in case of hysteresis loops of ferromagnets, where the minor loop area is related to the volume fraction [28]. However, in the absence of any theoretical framework for deducing the phase fraction from bulk measurements, our assumption here is simpler and we take the normalized area of MHL directly as the phase fraction. More theoretical work is now required to establish the actual relation between the phase fraction and the area of MHL.

The increasing area of MHL during cooling represents the increasing phase fraction of the AFM phase. However, for simplicity, we shall always discuss in terms of the increase and decrease of the fraction of the FM phase. So unity minus the normalized area of MHL during the cooling cycle represents the decrease of the FM fraction and thus can be plotted on the same scale as that of the growing FM fraction.

Figure 4 shows the phase fraction of the FM phase as a function of temperature both while heating and cooling the sample. The temperature dependent phase fraction very closely resembles the famous 'S' shaped transformation-time curve which is predicted by the Avrami model [15]. The shape of the curve enables us to fit the phase fraction with an equation very similar to the KJMA equation by replacing time with temperature.

$$f = 1 - \exp(-k(T - T_0)^{\eta}) \tag{3}$$

where T_0 is the onset temperature of the transformation. The values of T_0 and η on the heating cycle are 260 and 1.837 respectively. Similarly on the cooling cycle, the values of T_0 and η are 239.6 and 1.324 respectively. As can be clearly

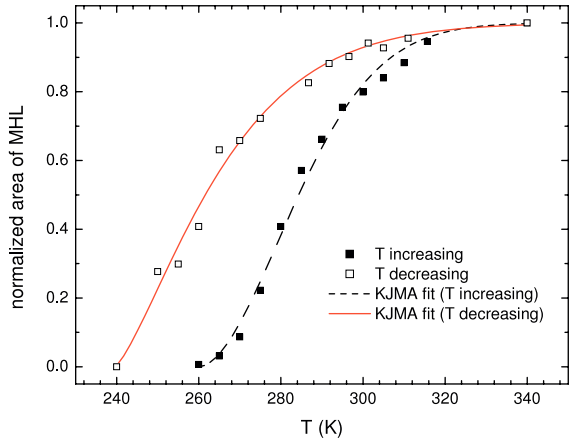

Figure 4. Temperature dependence of the areas of MHLs inferred from the ac susceptibility measurements shown in figure 1. The areas of MHLs are related to the phase fraction of the ferromagnetic phase. See text for details for the estimation of phase fraction during both the heating and cooling cycles. The dashed line shows the theoretical curve for the heating cycle following equation (3). Similarly, the solid line indicates the theoretical curve using the same equation for the cooling cycle.

seen, the experimental data can be very well described with this law. This close similarity indicates the growth kinetics across a first order transition follow some kind of universal behaviour irrespective of the detailed nature of the phases involved. Similar to our observation, it has been shown that the extended Avrami model can also be applied to describe the volume fraction of the reversed domains in ferroelectrics subjected to oscillating electric fields [29].

Similar arguments can be carried out for the field induced (metamagnetic) transition. Figure 5 shows the isothermal magnetization at $T = 220$ K. This temperature value was chosen so that the entire sample is definitely single phase AFM. A sharp rise in magnetization at about 4 T on the field-increasing curve marks the onset of the AFM to FM transition. The transition is not complete until 8 T, which is quite close to the upper limit of magnetic field in our VSM. On decreasing the field, we see a hysteresis across the transition similar to the temperature dependent ac susceptibility measurement. This indicates that the metamagnetic transition is also of a first order nature. The presence of phase coexistence across the metamagnetic transition can be seen by generating MHLs on the field-increasing and field-decreasing cycles. Figure 5(a) shows a few representative MHLs initiated on the field-increasing cycle. Similarly, figure 5(b) shows MHLs initiated on the field-decreasing cycle.

Similar to the relaxation measurements in constant field which are shown in figure 2, isothermal time dependent magnetization measurements clearly show the presence of metastable states across the metamagnetic transition (see figure 6). Figure 6(a) shows the time dependent magnetization during the field-increasing cycle, whereas figure 6(b) shows relaxation during the field-decreasing cycle. Like the constant-field relaxation shown in figure 2, the isothermal relaxation at various fields also obeys the same law as expressed in equation (1).

The value of exponent at various fields during both the field-increasing and decreasing cycle is shown in figure 7. The same behaviour of the exponent is again seen here across the field induced transition. This shows that the transition kinetics appear to be the same for both the temperature and field induced transitions.

Figure 8 shows the areas of MHLs during the metamagnetic transition along with the theoretical fit given by the equation:

$$f = 1 - \exp(-k(H - H_0)^{\eta}). \tag{4}$$

This is just equation (3) rewritten by replacing T with H. The phase fraction again closely follows the Avrami law as can be seen from figure 8. Here the values of H_0 and η are 30 000 and 2.284 respectively on the field-increasing cycle. The values of H_0 and η are 12 856 and 2.198 respectively on the field-decreasing cycle. The difference in the values of η for the temperature driven transition (see equation (3)) and the field driven transition probably arises because the dependence of the activation energy on the magnetic field and temperature are not explicitly included in the above equations. Further work is needed to establish a generalized function similar to the case of

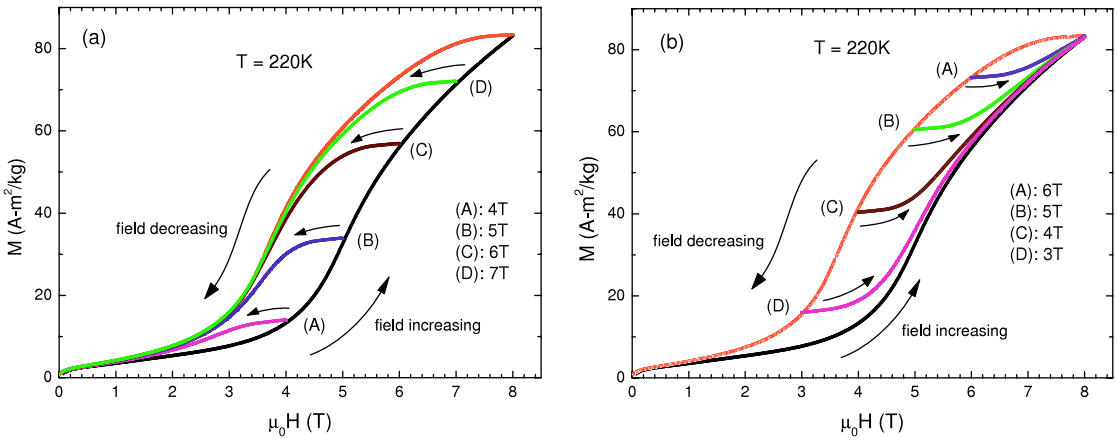

Figure 5. Isothermal magnetization as a function of temperature. Minor hysteresis loops (a) on the field-increasing cycle and (b) on the field-decreasing cycle. The field values of initiation of minor loops are marked as A, B, C and D.

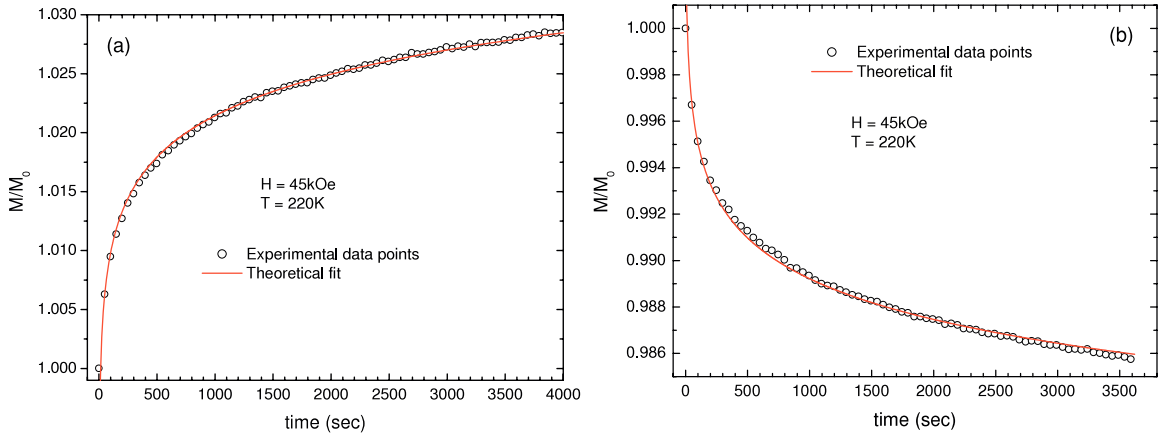

Figure 6. Time dependent magnetization during the field induced transition at representative fields on (a) the field-increasing cycle and (b) the field-decreasing cycle. The solid line indicates the calculated curve using equation (1).

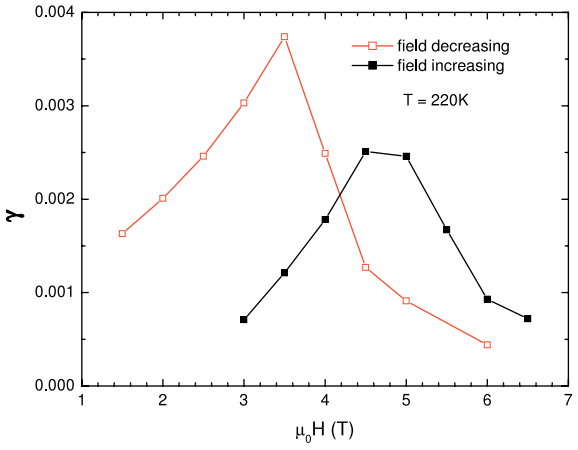

Figure 7. Field dependence of the exponent γ in equation (1) during the field induced transition. The absolute value of γ is plotted for the field-decreasing cycle on the same scale for the sake of comparison.

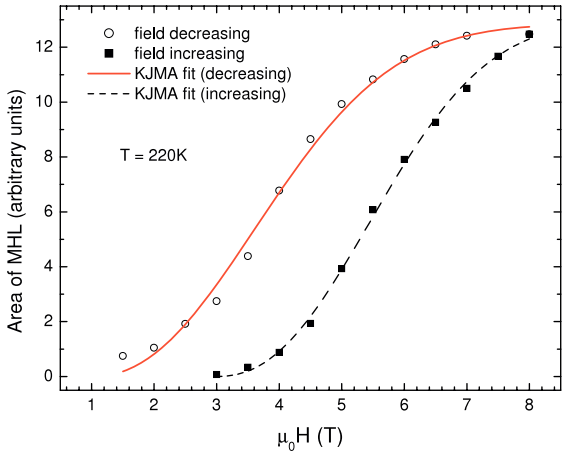

Figure 8. Field dependence of areas of MHLs inferred from the isothermal magnetization measurements shown in figure 5, which is related to the phase fraction of the ferromagnetic phase. See text for details for the estimation of phase fraction during both the field-increasing and field-decreasing cycles. The dashed line shows the theoretical curve for the field-increasing cycle following equation (4). Similarly, the solid line indicates the theoretical curve using the same equation for the field-decreasing cycle.

electric field driven reversal of domains in ferroelectrics [29]. The areas of MHLs are represented in arbitrary units as we do not have a complete envelope curve whose area can be taken for normalization. We thus see that the temperature and field driven transitions both follow similar kinetics and have a very close resemblance to that of phase transformation during the solidification process. We hope our experimental results will provide a path for future work on identifying the phase fraction from bulk measurements and also to explain transformation kinetics in a generalized manner. More experimental and theoretical work is required on various systems undergoing a first order phase transition before a generalized framework can be established.

4. Conclusion

In conclusion, we have studied the bulk ac susceptibility and dc magnetization across the antiferromagnetic to ferromagnetic transition in $(Fe_{0.975}Ni_{0.025})_{50}Rh_{50}$. The time dependent magnetization during both the temperature and field driven transitions follows a power law which is thought to arise from the long-range dipolar interaction between the ferromagnetic clusters. The exponent of the power law equation shows a non-monotonic behaviour in both the temperature and field induced transitions. This non-monotonic behaviour points towards a nucleation and growth behaviour very similar to the Avrami model of crystallization of solids. The areas of the minor hysteresis loops across the transition can be related to the phase fraction of the product phase involved in a first order transition. The evolution of these areas follow the law explained by the Avrami model, which is extended by replacing time with temperature and magnetic field. Further theoretical work is now required which can relate the parameters from bulk magnetization measurements to the phase fraction across a first order magnetic transition.

Acknowledgment

We thank Mrs Pragya Tiwari for helping us with the EDS measurements.

References

[1] Christian J W 2002 *The Theory of Transformations in Metals and Alloys* 3rd edn (Amsterdam: Pergamon)
[2] Zeldov E, Majer D, Konczykowski M, Geshkenbein V B, Vinokur V M and Shtrikman H 1995 *Nature* **375** 373
[3] Manekar M, Mukherjee C and Roy S B 2007 *Europhys. Lett.* **80** 17004
[4] Wu W, Israel C, Hur N, Park S, Cheong S and Lozanne A 2006 *Nat. Mater.* **5** 881
[5] Moore J D, Perkins G K, Bugoslavsky Y, Cohen L F, Chattopadhyay M K, Roy S B, Chaddah P, Gschneidner K A Jr and Pecharsky V K 2006 *Phys. Rev.* B **73** 144426
[6] Roy S B, Perkins G K, Chattopadhyay M K, Nigam A K, Sokhey K J S, Chaddah P, Caplin A D and Cohen L F 2004 *Phys. Rev. Lett.* **92** 147203
[7] Murakami Y, Yoo J H, Shindo D, Atou T and Kikuchi M 2003 *Nature* **423** 965
[8] Zhang L, Israel C, Biswas A, Greene R L and Lozanne A 2002 *Science* **298** 805
[9] Renner C, Aeppli G, Kim B G, Soh Y A and Cheong S W 2002 *Nature* **416** 518
[10] Uehara M, Mori S, Chen C H and Cheong S W 1999 *Nature* **399** 560
[11] Soibel A, Zeldov E, Rappaport M, Myasoedov Y, Tamegai T, Ooi S, Konczykowski M and Geshkenbeink V B 2000 *Nature* **406** 282
[12] White R M and Geballe T H 1979 *Long Range Order in Solids* (New York: Academic)
[13] Manekar M, Roy S B and Chaddah P 2000 *J. Phys.: Condens. Matter* **12** L409
[14] Granados X, Fontcuberta J, Obradors X and Torrence J B 1992 *Phys. Rev.* B **46** 15683
[15] Avrami M 1939 *J. Chem. Phys.* **7** 1103
[16] Annaorazov M P, Nikitin S A, Tyurin A L, Asatryan K A and Dovletov A K 1996 *J. Appl. Phys.* **79** 1689
[17] Nikitin S A, Myalikgulyev G, Annaorazov M P, Tyurin A L, Myndyev R W and Akopyan S A 1992 *Phys. Lett.* A **171** 234
[18] Ibarra M R and Algarabel P A 1994 *Phys. Rev.* B **50** 4196
[19] Algarabel P A, Ibarra M R, Marquina C, Moral A D, Galibert J, Iqbal M and Askenazy S 1995 *Appl. Phys. Lett.* **66** 3061
[20] Kouvel J S and Hartelius C C 1962 *J. Appl. Phys.* **33** (suppl.) 1343
[21] Zakharov A I, Kadomtseva A M, Levitin R Z and Ponyatovskii E G 1964 *Sov. Phys.—JETP* **19** 1348
[22] Baranov N V and Barabanova E A 1995 *J. Alloys Compounds* **219** 139
[23] Yuasa S, Miyajima H and Otani Y 1994 *J. Phys. Soc. Japan* **63** 3129
[24] Manekar M and Roy S B 2008 *Euro. Phys. J.* B (at press)
[25] Chaikin P M and Lubensky T C 1995 *Principles of Condensed Matter Physics* (Cambridge: Cambridge University Press) see chapter 4
[26] Sokhey K J S, Manekar M, Chattopadhyay M K, Kaul R, Roy S B and Chaddah P 2003 *J. Phys. D: Appl. Phys.* **36** 1366
[27] Sampaio L C, Hyndman R, de Menezes F S, Jamet J P, Meyer P, Gierak J, Chappert C, Mathet V and Ferre J 2001 *Phys. Rev.* B **64** 184440
[28] Jiles D C 1992 *IEEE Trans. Magn.* **28** 2602
[29] Orihara H, Hashimoto S and Ishibashi Y 1994 *J. Phys. Soc. Japan* **63** 1031